Correlation and Large-Scale Simultaneous Significance Testing

Bradley Efron

Abstract

Large-scale hypothesis testing problems, with hundreds or thousands of test statistics "z_i" to consider at once, have become familiar in current practice. Applications of popular analysis methods such as false discovery rate techniques do not require independence of the z_i's, but their accuracy can be compromised in high-correlation situations. This paper presents computational and theoretical methods for assessing the size and effect of correlation in large-scale testing. A simple theory leads to the identification of a single omnibus measure of correlation. The theory relates to the correct choice of a null distribution for simultaneous significance testing, and its effect on inference.

1. Introduction   Modern computing machinery and improved scientific equipment have combined to revolutionize experimentation in fields such as biology, medicine, genetics, and neuroscience. One effect on statistics has been to vastly magnify the scope of multiple hypothesis testing, now often involving thousands of cases considered simultaneously. The cases themselves are typically of familiar form, each perhaps a simple two-sample comparison, but with their test statistics correlated in some unknown fashion. This paper concerns the effect of correlation on multiple testing procedures, particularly false discovery rate techniques, Benjamini and Hochberg (1995).

Test statistics from two microarray experiments are displayed in Figure 1. The experiments, described in Section 2, reported two-sample t-statistics "t_i" comparing expression levels under two different conditions for N genes, $N = 3226$ for the breast cancer study in the left panel, and $N = 7680$ for the HIV experiment on the right. The t_i's have been converted to z-values for easy analysis later,

$$z_i = \Phi^{-1}(G_0(t_i)), \qquad i = 1, 2, \dots, N, \tag{1.1}$$

where Φ is the standard normal cumulative distribution function (cdf), and G_0 is a putative null cdf for the t-values. G_0 was taken to be a standard student's t cdf with appropriate degrees of freedom for the HIV study, while a permutation method described in Section 4 provided G_0 for the breast cancer experiment (also nearly a student's t cdf.) Assuming G_0 is the correct null distribution for t_i, transformation (1.1) yields
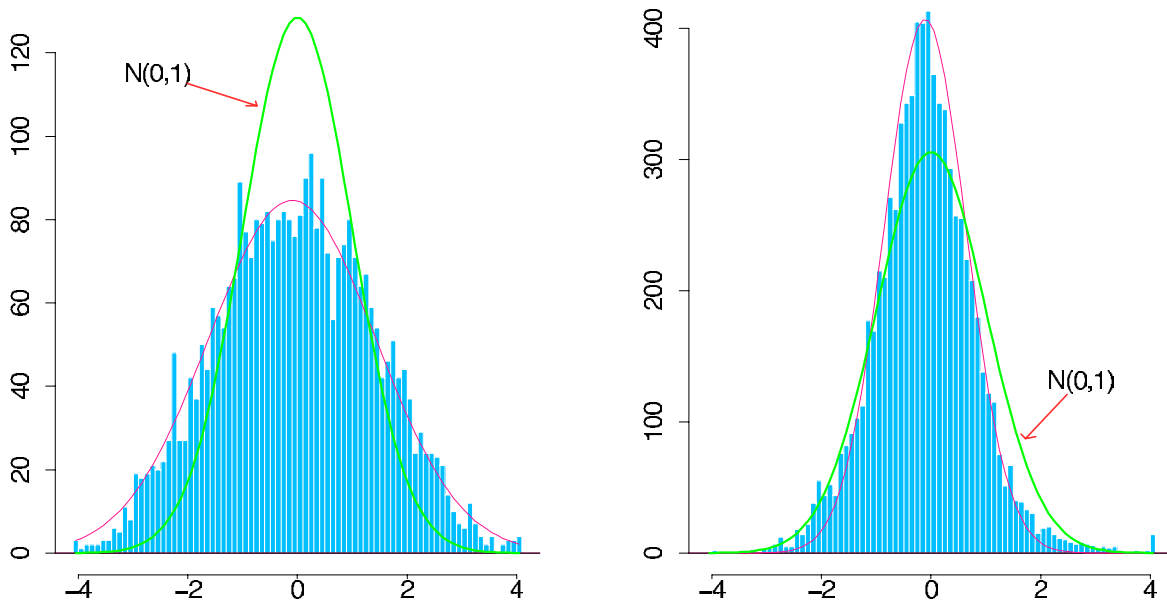
$$z_i \sim N(0, 1) \tag{1.2}$$

Figure 1: Histograms of z-values from two microarray experiments . *Left panel*: breast cancer study, 3226 genes; *Right panel* HIV study, 7680 genes. *Heavy curves* indicate $N(0,1)$ theoretical null densities; *Light curves* indicate empirical null densities fit to central z-values, as in Efron (2004). The theoretical null distributions are too narrow in the left panel and too wide in the right. Both effects can be caused by correlations among the null z-values. Data from Hedenfalk et al. (2001), left panel, and van't Wout et al. (2003), right.

for the null cases, called the *theoretical null* in what follows. Form (1.2) for the null distri- bution is convenient for general discussion, and can be achieved, or at least approximated, in most testing situations via transformations like (1.1).

Microarray experiments usually presuppose most of the genes to be null, the goal being to identify a small subset of interesting non-null genes for future study, so we expect $N(0,1)$ to fit the center of the z-value histogram. This is not the case in Figure 1, where $N(0,1)$ is too narrow for the breast cancer histogram and too wide for the HIV data.

This paper concerns two related results:

(1) Correlation can cause effects like those seen in Figure 1, considerably widening or narrowing the distribution of the null z-values.

(2) These effects have substantial impact on simultaneous significance testing, and must be accounted for in deciding which cases should be reported as non-null.

Sections 2 and 3 begin with a normal-theory analysis of z-value correlations. A sur-

prisingly simple result emerges, in which the effect of all the pair-wise correlations, several million of them for Figure 1's examples, is summarized in a single omnibus measure. Section 4 replaces normal theory with permutation methods, carried out in detail for the breast cancer data, showing nice agreement with the theory.

The effect of correlation on simultaneous inference is discussed in Section 5, particularly in terms of false discovery rates (Fdr). Broadly speaking, a wide central histogram like that for the breast cancer data implies more null z-values in the tails, so that significance levels judged according to the theoretical $N(0,1)$ null will be too liberal. Conversely, the theoretical null is too conservative for the HIV data. This provides some support for the use of an *empirical null* distribution, a normal curve fit to the central portion of the z-value histogram, Efron (2004, 2005). The light curves in Figure 1 are empirical nulls.

$$breast\ cancer: N(-0.09, 1.55^2) \qquad HIV: N(-0.11, 0.75^2). \tag{1.3}$$

There is nothing subtle about the inferential effects of correlation. Factors of seven or more on estimated false discovery rates are common in reasonable scenarios, as shown in Section 5. Other simultaneous inference methods seen just as vulnerable as Fdr techniques, the latter being featured here only because of their simple structure.

Three pertinent references are mentioned in the discussion that follows: Qui, Klebanov, and Yakovlev (2005), Qui et al. (2005), and Owen (2005). Permutations and correlated z-values also play a role in Westfall and Young's theory of adjusted p-values (1993), Westfall (1997), and Ge, Dudoit, and Speed (2003), but with less direct bearing on the ideas here. A brief discussion and some remarks conclude the paper.

2. Correlation Effects on the Null Distribution   We begin with a normal-theory analysis for the effects of correlation on the null distribution of z-values. For these calculations it is assumed that *all* cases are null,

$$z_i \sim N(0,1) \text{ for } i = 1, 2, \dots, N, \tag{2.1}$$

so that the theoretical $N(0,1)$ null distribution is individually correct. Nevertheless it will turn out that correlation among the z_i's can make the null distribution effectively wider or narrower than $N(0,1)$, as in Figure 1. Section 5 shows that in real problems, where we hope to detect some non-null cases, correlation effects can play a major role in their correct identification.

Here is a thumbnail description of the studies featured in Figure 1, along with some of the notation used in what follows. The breast cancer study compared gene activity in 15

patients observed to have one of two different genetic mutations known to increase breast cancer risk, "BRCA1" or "BRCA2", Hedenfalk et al. (2001). It included 7 BRCA1 and 8 BRCA2 women, each providing a microarray of expression levels on the same $N = 3226$ genes. The usual two-sample t-statistic "t_i" comparing BRCA2 versus BRCA1 for the 15 gene i expression levels gave z_i as in (1.1), with G_0 nearly a student's t-distribution with 13 degrees of freedom. Similarly, the HIV study compared four HIV positive patients versus four HIV negative controls, $N = 7680$ genes per microarray, van't Wout et al. (2003). In this case G_0 was taken to be student's t with 6 degrees of freedom. These data sets are discussed further in Efron (2004, 2005).

Let X represent the full data set, for example an N by n matrix for the breast cancer study, having $N = 3226$ rows corresponding to genes and $n = 15$ columns corresponding to microarrays. There each row of X yielded a t statistic t_i and then a z-value z_i as in (1.1), with $\mathbf{z}$ representing the vector of all N z_i's. **Note** It is not necessary that the z_i's be obtained from t-tests, only that null distribution (2.1) can be achieved or approximated. For example, each of the original N cases might involve a separate linear regression, with the ith case yielding p-value p_i for some parameter of special interest, and $z_i = \Phi^{-1}(p_i)$.

It is helpful to work with histogram counts rather than with the vector of z-values itself. Each histogram in Figure 1 has its z-axis partitioned into $K = 82$ bins of width $\Delta = 0.1$, running from -4.1 to 4.1. We denote the count vector by $\mathbf{y}$,

$$y_k = \#\{z_i \text{ in } k^{\text{th}} \text{ bin}\}, \qquad k = 1, 2, \dots, K; \tag{2.2}$$

$\mathbf{y}$ is essentially the order statistic of $\mathbf{z}$, exactly so if we let $\Delta \to 0$. Methods like False Discovery Rates depend only on the ordered z-values.

The histogram counts y_k arise from a partition of $\mathcal{Z}$, the sample space for the z-values, into K bins,

$$\mathcal{Z} = \cup_{k=1}^{K} \mathcal{Z}_k, \tag{2.3}$$

each bin being of width Δ, with center-point "$z[k]$". The following definitions lead to useful representations for the mean and covariance of $\mathbf{y}$:

$$\pi_k(i) = Pr\{z_i \in \mathcal{Z}_k\}, \quad \pi_{k\cdot} = \frac{\sum_{i=1}^{N} \pi_k(i)}{N}, \tag{2.4}$$

and

$$\gamma_{k\ell}(i,j) = Pr\{z_i \in \mathcal{Z}_k \quad \text{and} \quad z_j \in \mathcal{Z}_\ell\}, \qquad \gamma_{k\ell\cdot} = \frac{\sum_{i \neq j} \gamma_{k\ell}(i,j)}{N(N-1)}. \tag{2.5}$$

4

Because of assumption (2.1) all the $\pi_k(i)$ values are determined by $\varphi(z)$, the standard normal density, with Taylor approximation around centerpoint $z[k]$

$$\pi_{k.} = \pi_k(i) \doteq \Delta \cdot \varphi(z[k]) \qquad (\varphi(z) = e^{-\frac{1}{2}z^2}/\sqrt{2\pi}). \tag{2.6}$$

The *expectation vector* $\boldsymbol{\nu} = (v_1, v_2, \ldots, v_K)'$ of $\mathbf{y}$ is determined by (2.1),

$$\boldsymbol{\nu} = N\boldsymbol{\pi}_{.} \doteq (\cdots, N\Delta\varphi(z[k]), \cdots)'. \tag{2.7}$$

Definitions (2.4-2.5) lead to a convenient expression for the covariance matrix of $\mathbf{y}$;

Lemma 1

$$\mathrm{Cov}(\mathbf{y}) = C_0 + C_1 \tag{2.8}$$

where C_0 is the multinomial covariance matrix that would apply if the z-values were independent,

$$C_0 = \mathrm{diag}(\boldsymbol{\nu}) - \boldsymbol{\nu}\boldsymbol{\nu}'/N = N[\mathrm{diag}(\boldsymbol{\pi}_{.}) - \boldsymbol{\pi}_{.}\boldsymbol{\pi}_{.}'], \tag{2.9}$$

and

$$C_1 = \left(1 - \frac{1}{N}\right)\mathrm{diag}(\boldsymbol{\nu})\boldsymbol{\delta}\,\mathrm{diag}(\boldsymbol{\nu}) \qquad \text{with } \delta_{k\ell} = \gamma_{k\ell.}/\pi_{k.}\pi_{\ell.} - 1. \tag{2.10}$$

Here "diag" indicates a diagonal matrix and $\boldsymbol{\pi}_{.} = (\pi_{1.}, \pi_{2.}, \ldots, \pi_{K.})'$.

Proof   Let $I_k(i)$ be the indicator function for event $z_i \in \mathcal{Z}_k$, so $y_k = \sum_{i=1}^{N} I_k(i)$ and for $k \neq \ell$

$$E\{y_k y_\ell\} = E\left\{\sum_{i\neq j} I_k(i)I_\ell(j)\right\} = \sum_{i\neq j} \gamma_{k\ell}(i,j)$$
$$= N(N-1)\gamma_{k\ell.} \tag{2.11}$$

Then

$$\mathrm{cov}(y_k, y_\ell) = N(N-1)\gamma_{k\ell.} - N^2\pi_{k.}\pi_{\ell.}$$
$$= -N\pi_{k.}\pi_{\ell.} + N(N-1)(\gamma_{k\ell.} - \pi_{k.}\pi_{\ell.}). \tag{2.12}$$

Similarly,

$$\mathrm{var}(y_k) = N(\pi_{k.} - \pi_{k.}^2) + N(N-1)(\gamma_{kk.} - \pi_{k.}^2), \tag{2.13}$$

verifying Lemma 1   ■

If z_i and z_j are independent in (2.1) then $\gamma_{k\ell}(i,j) = \pi_k(i)\pi_\ell(j)$; independence of all z-values implies that all the elements of matrix $\boldsymbol{\delta}$ in (2.10) are zero, leaving $\mathrm{cov}(\mathbf{y}) = C_0$. Conversely, the amount of correlation between the z-values determines the size of $\boldsymbol{\delta}$ and the increase of $\mathrm{cov}(\mathbf{y})$ above C_0.

To approximate $\boldsymbol{\delta}$, we add the assumption of bivariate normality for any pair of z-values, $\mathrm{cov}(z_i, z_j) \equiv \rho_{ij}$, so that as in (2.6),

$$\gamma_{k\ell}(i,j) \doteq \frac{\Delta^2}{2\pi\sqrt{1-\rho_{ij}^2}} \, \exp\left\{ -\frac{1}{2} \frac{z[k]^2 - 2\rho_{ij}z[k]z[\ell] + z[\ell]^2}{1-\rho_{ij}^2} \right\}, \qquad (2.14)$$

Letting $g(\rho)$ indicate the empirical density of the $N(N-1)$ correlations ρ_{ij}, and using (2.6)-(2.14) yields a useful approximation:

Lemma 2   Under the bivariate normal approximation (2.14), the matrix $\boldsymbol{\delta}$ in (2.10) has elements

$$\delta_{k\ell} \doteq \int_{-1}^{1} \left[\frac{1}{\sqrt{1-\rho^2}} \exp\left(\frac{\rho}{2(1-\rho^2)} \{2z[k]z[\ell] - \rho(z[k]^2 + z[\ell]^2)\} \right) - 1 \right] g(\rho)d\rho. \qquad (2.15)$$

(This compares with Theorem 1 in Owen (2005); the assumptions there imply the bivariate normal condition (2.14).)

Application of Lemmas 1 and 2 requires an estimate of the correlation density $g(\rho)$, which we can obtain from observed correlations between the rows of X. As described in Remark A of Section 7, this gave

$$breast\ cancer: \quad g(\rho) \overset{.}{\sim} N(0, 0.153^2) \qquad (2.16)$$

for the breast cancer data, and, more roughly,

$$HIV: \ g(\rho) \overset{.}{\sim} N(0, 0.42^2), \qquad (2.17)$$

for the HIV study. It is no accident that $g(\rho)$ has mean near zero; in both cases the data matrix X had its columns standardized to mean zero and variance one, usual practice to negate "brightness" disparities between microarrays, see Bolstad et al. (2003) and Qui et al. (2005). This forces the sum of covariances, and, nearly, the sum of correlations, to be zero. The normality assumed in (2.16) is not crucial, see Remark B. Section 3 shows that the standard deviation 0.153 is the vital number. Remark E discusses what happens in the absence of standardization.

Approximation (2.16) indicates a substantial amount of global correlation among genes in the breast cancer study, and even more correlation for the HIV study (2.17). The five examples in Owen's (2005) Table 1 had standard deviations for $g(\rho)$ between 0.17 and 0.26, as did Qui et al.'s (2005) main example. It is not surprising that correlations of this magnitude

	Independent	C_{norm}	C_{perm}	Poisson
$sd(Y_0)$:	26.4	**171.4**	176.0	176.4
$sd(Y_1)$:	4.5	**16.1**	14.9	14.7
$cor(Y_0, Y_1)$:	(-0.12)	**(-0.89)**	(-0.81)	(-0.90)

Table 1: Standard deviations and correlations for central and tail counts (Y_0, Y_1), (2.19); $z_i \sim N(0,1)$ $i = 1, 2, \ldots, 3226$; for z_i's independent or z_i's correlated as in C_{norm}, (2.18); also for permutation covariance C_{perm}, (4.2). C_{norm} and C_{perm} produce much larger standard deviations and much more negative correlations. "Poisson" calculated from Poisson approximation model (3.15).

can undercut standard inference techniques, the key message in Qui et al. The goal here, made explicit in Section 5, is to understand and correct correlational problems.

Substituting (2.16) into (2.15) and then into Lemma 1, gives estimated null hypotheses covariance matrix "C_{norm}",

$$\mathrm{cov}(\mathbf{y}) = C_{\mathrm{norm}} \tag{2.18}$$

for the breast cancer data. The correlation term C_1 in $\mathrm{cov}(\mathbf{y}) = C_0 + C_1$, (2.8), dominates the independence term C_0. As an informative example we will use later, define

$$Y_0 = \#\{z_i \in [-1, 1]\} \quad \text{and} \quad Y_1 = \#\{z_i \geq 2.5\}, \tag{2.19}$$

these being central and tail counts for a hypothetical null vector $\mathbf{z}$ satisfying (2.1). Table 1 shows standard deviations and correlation for Y_0 and Y_1 if the z_i's are independent, or if they are correlated such that $\mathrm{cov}(\mathbf{y}) = C_{\mathrm{norm}}$. (Table 1 can be computed from $\mathrm{cov}(\mathbf{y})$ since Y_0 and Y_1 are linear functions of $\mathbf{y}$). Results for C_{perm}, the permutation estimate from Section 4, agree with C_{norm}. The cutoffs ± 1 and 2.5 in (2.19) were chosen for convenient exposition, and could just as well be replaced by similar values, say ± 0.75 and 3.0.

We see that gene correlations have a powerful effect on the counts that would be observed under null hypothesis (2.1): standard deviations are multiplied several fold (this being the main point in Owen (2005)), while the negative correlation between the central and tail counts is driven toward -1. Tail null counts play a crucial role in computing false discovery rates, as discussed in Section 5 where the extreme negative correlation between Y_0 and Y_1 is used to "condition" Fdr estimates. Section 3 provides an explanation for the negative correlation.

3. First Eigenvector   Lemmas 1 and 2 decompose the covariance matrix of the count

vector **y** into an independence term C_0 and an additional term C_1 that accounts for correlation among the z-values, (2.8). This section presents a simple approximation to C_1 in terms of its first eigenvector, which will be used in Sections 4 and 5 to explain the effects of correlation on simultaneous inference.

The smooth curve in Figure 2 is the first eigenvector of C_{norm}, (2.16)-(2.18) the normal-theory estimate of $\text{cov}(\mathbf{y})$ for the breast cancer data, while the jagged curve is the corresponding quantity for the permutation-based estimate C_{perm} of Section 4. The dots indicate the first eigenvector of C_{norm} for the HIV data, using (2.17). All three curves exhibit the same "wing-shaped" form. This will turn out to be proportional to

$$w(z) \equiv \varphi(z)\frac{z^2 - 1}{\sqrt{2}} = \varphi''(z)/\sqrt{2}, \tag{3.1}$$

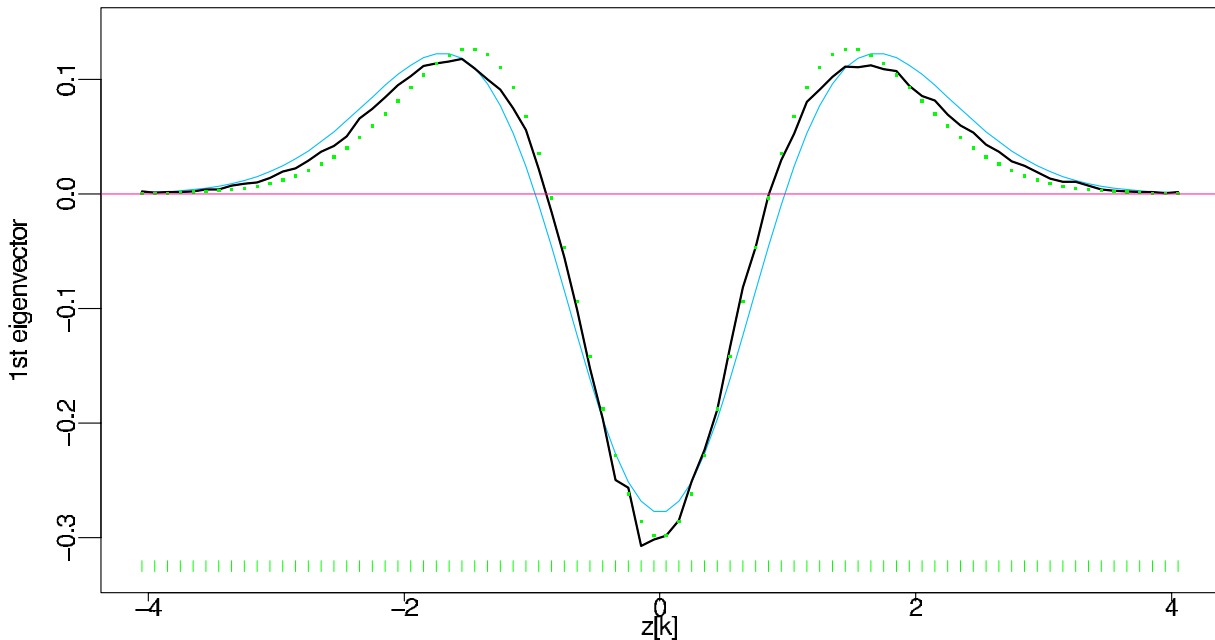where $\varphi(z)$ is the standard normal density, (2.6).

Figure 2: First eigenvectors of three different estimates of $\text{cov}(\mathbf{y})$: *smooth curve* normal-theory estimate (2.18) for breast-cancer data; *dots* normal-theory estimate for HIV data (2.17); *jagged curve* permutation estimate for breast cancer data (4.2); The striking "wing-shaped" form is proportional to the second derivative of the standard normal density. Dashes indicate bin midpoints $z[k]$.

We use notation (2.3)-(2.6), and work in the discretized framework of Lemmas 1 and 2:

Lemma 3   Suppose $g(\rho)$, the correlation density in (2.15) has mean zero and standard

deviation

$$\alpha = \left[\int_{-1}^{1} \rho^2 g(\rho) d\rho \right]^{\frac{1}{2}}. \tag{3.2}$$

Then the matrix $\boldsymbol{\delta}$ in (2.10) is approximated by the outer product

$$\boldsymbol{\delta} \doteq \alpha^2 \mathbf{q} \mathbf{q}' \quad \text{where} \quad q_k = \frac{z[k]^2 - 1}{\sqrt{2}}, \tag{3.3}$$

with $z[k]$ the centerpoint of the kth histogram bin, $k = 1, 2, \ldots, K$; approximation (3.3) becomes exact as $\alpha \to 0$.

Proof   Let $R_{k\ell}(\rho)$ be the integrand in (2.15),

$$R_{k\ell}(\rho) = \frac{1}{\sqrt{1-\rho^2}} \exp\left\{ \frac{\rho}{1-\rho^2} \, z[k]z[\ell] - \frac{1}{2} \frac{\rho^2}{1-\rho^2} (z[k]^2 + z[\ell]^2) \right\} - 1. \tag{3.4}$$

Expanding $R_{k\ell}(\rho)$ in a Taylor series around $\rho = 0$, and ignoring terms of order ρ^3 or higher, gives

$$R_{k\ell}(\rho) \doteq \rho z[k]z[\ell] + \rho^2 q_k q_\ell; \tag{3.5}$$

then, since $g(\rho)$ has mean 0,

$$\delta_{k\ell} = \int_{-1}^{1} R_{k\ell}(\rho) g(\rho) d\rho \doteq \alpha^2 q_k q_\ell, \tag{3.6}$$

which is (3.3).   ∎

Combining the three lemmas yields a useful approximation for the null covariance matrix of the count vector $\mathbf{y}$ under the bivariate normal assumptions of Section 2:

Theorem   If $g(\rho)$ has mean 0 and standard deviation α, then

$$\text{cov}(\mathbf{y}) \doteq [\text{diag}(\boldsymbol{\nu}) - \boldsymbol{\nu}\boldsymbol{\nu}'/N] + \left(1 - \frac{1}{N}\right)(\alpha \mathbf{W})(\alpha \mathbf{W})' \tag{3.7}$$

Here $\boldsymbol{\nu} = E\{\mathbf{y}\}$ as in (2.7), while $\mathbf{W}$ has components

$$W_k = N\Delta\varphi(z[k])\frac{z[k]^2 - 1}{\sqrt{2}} = N\Delta w(z[k]), \tag{3.8}$$

with $w(\cdot)$ the wing-shaped function (3.1), N the number of cases, and Δ the bin width.

The Theorem helps explain Figure 2: the second term in (3.7) dominates $\text{cov}(\mathbf{y})$ in our two examples, making its first eigenvector nearly proportional to $w(z)$.

Table 2 relates to the accuracy of the Theorem. It shows the proportion of variance explained by the first eigenvector (i.e. first eigenvalue divided by sum of eigenvalues) for C_1,

the correlation term in (2.8), and also for $\text{cov}(\mathbf{y}) = C_0 + C_1$, assuming $g(\rho) \sim N(0, \alpha^2)$. For the breast cancer value $\alpha = 0.153$, the proportions are 98% for C_1, (the crucial quantity for the accuracy of (3.7)), and 45% for $C_\text{norm} = \text{cov}(\mathbf{y})$. $N = 3226$ in Table 2, but this choice has little effect on the numbers. The 98% proportion indicates the theorem's substantial accuracy in the breast cancer context. For the HIV data the proportion was 86%, still quite adequate.

α:	0	0.05	0.10	0.15	0.20	0.25	0.30
C_1:	1.00	1.00	0.99	0.98	0.97	0.95	0.90
C_norm:	.04	0.10	0.27	0.45	0.59	0.68	0.72

Table 2: Proportion of total variance explained by first eigenvector, as a function of α; for C_1, the correlation term in (2.8), and also for C_norm; assuming $g(\rho) \sim N(0, \alpha^2)$ and $N = 3226$. Proportions for C_1 determine accuracy of approximation (3.7).

The Theorem *summarizes the effect of* $\mathbf{z}$*'s entire correlation structure in a single parameter* α. This permits a relatively simple analysis of the inferential effects of correlation in what follows.

Poisson process considerations lead to a somewhat rough but evocative interpretation of the Theorem. Let $\mathbf{y} \sim Po(\mathbf{u})$ indicate a vector of independent Poisson variates, $y_k \overset{\text{ind}}{\sim} Po(u_k)$ for $k = 1, 2, \ldots, K$, while $\mathbf{y} \sim (\boldsymbol{\nu}, \Gamma)$ denotes that vector $\mathbf{y}$ has mean $\boldsymbol{\nu}$ and covariance Γ.

It is convenient here to consider the number of cases N to be a Poisson variate, say

$$N \sim Po(N_0), \tag{3.9}$$

with $N_0 = 3226$ in the breast cancer study. This slightly simplifies (3.7), to

$$\text{cov}(\mathbf{y}) \doteq \text{diag}(\boldsymbol{\nu}) + (\alpha \mathbf{W})(\alpha \mathbf{W})', \tag{3.10}$$

with $\boldsymbol{\nu}$ and $\mathbf{W}$ as in (2.7), (3.8) except that N_0 replaces N. If the z-values are independent then (3.9) makes the counts y_k independent Poisson variates,

$$\mathbf{y} \sim Po(\boldsymbol{\nu}), \tag{3.11}$$

agreeing with (3.10) at $\alpha = 0$.

A hierarchical model generalizes (3.11) to incorporate dependence. We assume that $\mathbf{y}$ depends on a mean vector $\mathbf{u}$, itself random,

$$\mathbf{y}|\mathbf{u} \sim \text{Po}(\mathbf{u}) \quad \text{where} \quad \mathbf{u} \sim (\boldsymbol{\nu}, \Gamma), \tag{3.12}$$

10

so that the components of $\mathbf{y}$ are conditionally independent given $\mathbf{u}$, but marginally dependent, with mean and covariance

$$\mathbf{y} \sim (\boldsymbol{\nu}, \ \mathrm{diag}\,(\boldsymbol{\nu}) + \Gamma). \tag{3.13}$$

To match (3.10) we need to set

$$\Gamma = (\alpha \mathbf{W})(\alpha \mathbf{W})', \tag{3.14}$$

Formulas (3.13)-(3.14) suggest a hierarchical Poisson structure for the count vector $\mathbf{y}$:

$$\mathbf{y} \sim Po(\mathbf{u}) \text{ where } \mathbf{u} = \boldsymbol{\nu} + A\mathbf{W}, \quad \text{with } A \sim (0, \alpha^2). \tag{3.15}$$

If $\alpha = 0$ this reduces to the independence case (3.11); otherwise the Poisson intensity vector $\boldsymbol{\nu}$ is modified by the addition of an independent random multiple "A" of $\mathbf{W}$ having standard deviation α.

Model (3.15) can only be an approximation since $\mathbf{u}$ may have negative coordinates, but it nicely explains phenomena like the extreme negative correlations between Y_0 and Y_1 seen in Table 1: vector $\mathbf{W}$ is negative in $[-1, 1]$ and positive elsewhere, as in Figure 2, so positive A in (3.15) decreases the central counts and increases the tail counts, (2.19), the opposite happening when A is negative. (The "Poisson" column of Table 1 was calculated from model (3.15), $\alpha = 0.153$ and $N = 3226$, except that the components of $\mathbf{u}$ were truncated at zero.)

Pursuing model (3.15) more carefully, the mean vector $\mathbf{u}$ turns out to be roughly proportional to a scaled normal density,

$$u_k \doteq \frac{N\Delta}{\sqrt{2\pi\sigma_A^2}} \exp\left\{ -\frac{z[k]^2}{2\sigma_A^2} \right\} \quad \text{with} \quad \sigma_A^2 = 1 + \sqrt{2}\,A, \tag{3.16}$$

see Remark D; (3.16) implies that positive A makes the counts behave in an overdispersed normal fashion compared to the theoretical $N(0,1)$ density, and conversely for A negative. This confirms the first main point of the Introduction: even if the null z-values are individually $N(0,1)$, correlation can make the ensemble $\mathbf{z}$ behave as $N(0, \sigma_A^2)$, with σ_A substantially different from 1. Section 4 shows the same phenomenon happening in a permutation analysis. This point is refined in Section 5, where it is shown that "A" can be estimated and used to condition simultaneous hypothesis tests.

4. Permutation Methods   The previous results depend upon the assumption of bivariate normality for every pair of z-values. Permutation methods lead to a direct empirical estimate "C_{perm}" for $\mathrm{cov}(\mathbf{y})$. Carried out here for the breast cancer data, C_{perm} agrees well with the

normal-theory estimate C_{norm}, (2.18), and lends support to the inferential theory of Section 5.

Let X represent the 3226×15 matrix of observed expressions. Each row of X, that is each gene, provides a two-sample t-statistic comparing the 8 BRCA2 and 7 BRCA1 expressions, $\mathbf{t}$ representing the vector of all 3226 t-values. Repeating the computation after a random permutation of the columns of X, that is after a random division of the patients into groups of 7 and 8, yields permuted matrix X^* and t-vector $\mathbf{t}^*$. 1000 such permutations were employed to estimate a permutation null distribution G_0 for the t-values, which turned out to be slightly shorter-tailed than a standard t variate with 13 degrees of freedom; z-values for the actual data were then calculated as in (1.1), $z_i = \Phi^{-1}(G_0(t_i))$, giving count vector $\mathbf{y}$:

$$
\begin{array}{ccccccc}
X & \longrightarrow & \mathbf{t} & \longrightarrow & \mathbf{z} & \longrightarrow & \mathbf{y} \\
3226 \times 15 & & 3226 & & 3226 & & 82
\end{array}
\tag{4.1}
$$

The permutations contain information beyond G_0. Each permuted data matrix X^* produces a count vector $\mathbf{y}^*$ according to (4.1). The sample covariance matrix of the 1000 $\mathbf{y}^*$'s,

$$
C_{\mathrm{perm}} = \sum_{b=1}^{1000} (\mathbf{y}^{*b} - \mathbf{y}^{*\cdot})(\mathbf{y}^{*b} - \mathbf{y}^{*\cdot})'/999 \quad [\mathbf{y}^{*\cdot} = \sum \mathbf{y}^{*b}/1000],
\tag{4.2}
$$

is a nonparametric estimate of the null covariance matrix for $\mathbf{y}$. By permuting entire microarrays we preserve the correlation structure of the genes while nullifying any actual BRCA1-BRCA2 differences. (*Note*: the matrix X in (4.1) had each gene's BRCA1 or BRCA2 average subtracted from its corresponding expression values in order to eliminate any genuine group differences from the permutation results.) Table 1 and Figure 2 demonstrate the similarity of C_{perm} to C_{norm}.

Each permutation vector $\mathbf{z}^*$ gave central and tail counts (Y_0^*, Y_1^*) as in (2.19). Figure 3 plots Y_1^* versus Y_0^*, now for 4000 permutations. The unconditional average of Y_1^* is 18.7, but that does not take into account the powerful covariate Y_0^*: in particular, for Y_0^* equaling the observed count 1570, a conditional expectation of about 118 is predicted. (Section 5 discusses why the observed central count might be so atypical of the permutation values in Figure 3.)

122 genes have z_i exceeding 2.5 for the breast cancer study. Does this collection of 122 genes deserve to be reported as "mostly non-null"? The answer obviously depends on whether the expected number of null genes having $z_i \geq 2.5$ is 18.7 or 118. Section 5 investigates this question, which bears on the second main point of the Introduction, the effect of correlation on simultaneous inference.
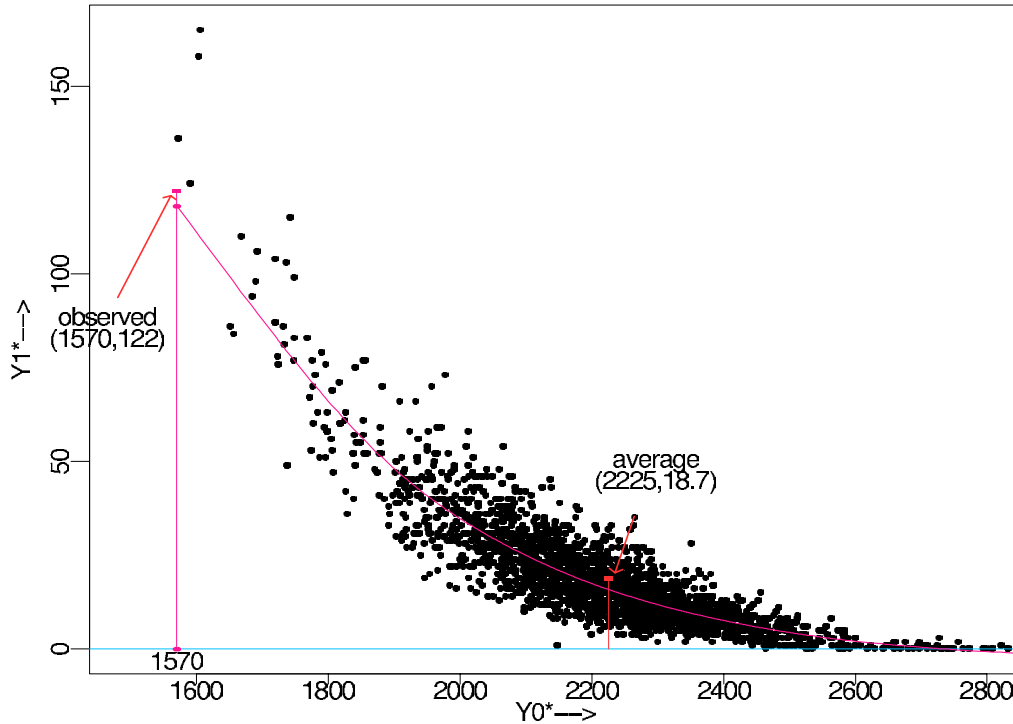
Figure 3: Central and tail counts (Y_0^*, Y_1^*) as in (2.19), for 4000 column-wise permutations of the breast cancer data; Y_1^* has unconditional expectation 18.7, but conditional expectation about 118 given Y_0^* equal to the observed central count 1570. Smooth curve is fitted smoothing spline..

The central count Y_0^* provides convenient estimates of standard deviation for $\mathbf{z}^*$, a permutation vector of N z-values,

$$\widehat{\sigma}_0^* = 1/\Phi^{-1}\left(\frac{1 + Y_0^*/N}{2}\right) \tag{4.3}$$

If we assume that the elements of $\mathbf{z}^*$ are normally distributed with mean 0 and some variance σ_0^{*2},

$$z_i^* \sim N(0, \sigma_0^{*2}), \tag{4.4}$$

then $E\{Y_0^*\} = N \cdot [2\Phi(1/\sigma_0^*) - 1]$ so (4.3) is a method of moment estimate for σ_0^* that depends only on the central count Y_0^*.

In Figure 4 the 4000 permutation $\mathbf{y}^*$ vectors have been averaged in groups having about the same central spread $\widehat{\sigma}_0^*$, (4.3); curve "1.2" is the log of the average of those $\mathbf{y}^*$ vectors having $1.15 \leq \widehat{\sigma}_0^* \leq 1.25$, etc. To first order the curves fall off as $-z^2/(2\sigma_0^2)$, with $\sigma_0 = 1.2, 1, 0.8$, i.e. as the log of a $N(0, \sigma_0^2)$ density. This agrees with theoretical result (3.16), where σ_A plays the role of σ_0, again showing how correlation can widen or narrow the effective

null distribution: those $\mathbf{y}^*$'s with large central spread put more null cases into the far tails, and conversely. Section 5 discusses how this phenomenon affects simultaneous significance testing, particularly false discovery rate methods.
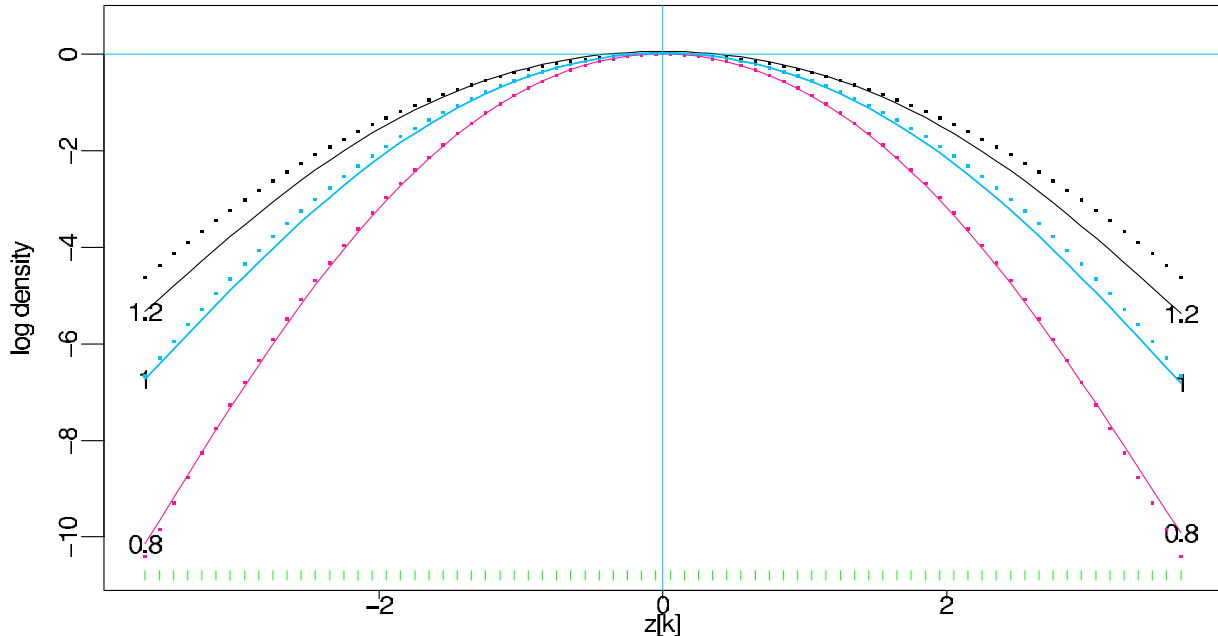

Figure 4:   Log average densities for the 4000 $\mathbf{y}^*$ vectors contributing to Figure 3; "1.2" graphs $\log \mathbf{y}_k^{*\cdot}$, from average of $\mathbf{y}^*$'s having $\widehat{\sigma}_0^*$ in $[1.15, 1.25]$, versus $z[k]$, etc. Dotted curves are $-.5z[k]^2/\sigma_0^2$ for $\sigma_0^2 = 1.2, 1.0, 0.8..$

5. Large-Scale Significance Testing   The scientific world is fond of significance testing because it requires a minimum of probabilistic modeling, no more than the specification of a null hypothesis distribution. However, as described in Sections 2.4, a disturbing danger arises in large-scale testing situations: correlations among the test statistics may substantially widen or narrow the effective null distribution. This section discusses the consequences of correlation effects on false discovery rates and other simultaneous testing techniques, as well as methods for connecting their inferences.

Suppose for a moment that we knew which z_i's among the full set of z-values correspond to null cases. For a given choice of x define

$$Y(x) = \#\{\text{null } z_i \geq x\} \quad \text{and} \quad T(x) = \#\{z_i \geq x\}. \tag{5.1}$$

Y_1 in (2.19) is $Y(2.5)$ in this notation, and $T(2.5) = 122$ for the breast cancer study. Lehman and Romano (2005) define the *false discovery proportion* to be

$$\text{Fdp}(x) = Y(x)/T(x), \tag{5.2}$$

assuming here that we are searching for "discoveries" in only the right tail. If $Fdp(x)$ were known (but not the identity of the null cases), say $Fdp(2.5) = 20/122 = 0.16$, the group of 122 genes could be reported as "mostly significant", with the assurance of producing only 16% false discoveries.

In practice $Y(x)$ is unobservable, and likewise $Fdp(x)$. A useful tactic is to replace $Y(x)$ by its expectation, as in Benjamini and Hochberg (1995), giving an estimated false discovery rate

$$Fdr(x) = E\{Y(x)\}/T(x). \qquad (5.3)$$

Benjamini and Hochberg's procedure actually involves the expected *ratio*

$$FDR(x) = E\{Y(x)/T(x)\}, \qquad (5.4)$$

ingeniously prescribing a data-based choice of x that controls the FDR below some preset value.

Our calculations will focus on $Fdr(x)$, (5.3), an observable ratio that is important and useful in its own right. $Fdr(x)$ is an empirical Bayes estimate of the *a posteriori* probability that case i is null given $z_i \geq x$, Storey (2002), Efron and Tibshirani (2002), amounting to a version of Storey's "q-value". Since $T(x)$ *is* observable, $Fdr(x)$ has intuitive interpretation as the expected proportion of null cases among those having $z_i \geq x$.

Formula (5.3) glosses over the fact that $E\{Y(x)\}$ itself is not directly calculable. Benjamini and Hochberg's original procedure replaced $E\{Y(x)\}$ with its upper bound assuming that all N cases were null, as in (2.1) where

$$E\{Y(x)\} = N \cdot \bar{\Phi}(x) \qquad [\bar{\Phi}(x) \equiv 1 - \Phi(x)]. \qquad (5.5)$$

Improvements on (5.5) are possible via estimation of "p_o", the proportion of null cases, Langaas et al. (2005), Storey et al. (2004), a point discussed later. For p_0 near 1.0, the preferred situation in microarray studies where the goal is to discover a small number of genuinely interesting genes, (5.5) is a good starting point for the discussion of correlation effects.

The hierarchical structure (3.15) gives conditional expectation

$$E\{\mathbf{y}|A\} = \boldsymbol{\nu} + A\mathbf{W} \qquad (5.6)$$

(using only $E\{\mathbf{y}|\mathbf{u}\} = \mathbf{u}$, not the full Poisson assumptions). Letting the bin width $\Delta \to 0$

in (2.7) and (3.8) produces a conditional version of (5.6), Remark H,

$$E\{Y(x)|A\} = N\bar{\Phi}(x)\left[1 + A\frac{x\varphi(x)}{\sqrt{2}\,\bar{\Phi}(x)}\right]. \tag{5.7}$$

The term multiplying A equals 4.99 at $x = 2.5$, giving conditional expectation $N\bar{\Phi}(x)[1.75]$ for $A = 0.15$, and $N\bar{\Phi}(x)[0.25]$ for $A = -0.15$.

Even such relatively modest values of A greatly affect the *conditional Fdr*

$$\mathrm{Fdr}(x|A) = E\{Y(x)|A\}/T(x), \tag{5.8}$$

which can be expressed as

$$\mathrm{Fdr}(x|A) = \mathrm{Fdr}_0(x)\left[1 + A\frac{x\varphi(x)}{\sqrt{2}\,\bar{\Phi}(x)}\right], \tag{5.9}$$

where $\mathrm{Fdr}_0(x)$ is the standard unconditional estimate $N\bar{\Phi}(x)/T(x)$. For $x = 2.5$, $\mathrm{Fdr}(x|A)$ varies by a factor of seven as A goes from -0.15 to +0.15. A principal point of this paper is that conditional Fdr estimates are available in situations like those of Figure 1, while the unconditional estimates can produce grossly misleading results.

The idea in what follows is that "A" in (5.9) or some equivalent parameter, can be estimated from the central spread of the histogram of z-values. We begin with a simple approach and then go on to more realistic procedures. Generalizing definition (2.19), for $x_0 > 0$ let

$$Y_0 = \#\{z_i \in [-x_0, x_0]\}. \tag{5.10}$$

and define

$$P_0 = 2\Phi(x_0) - 1 \qquad \text{and} \qquad Q_0 = \sqrt{2}x_0\varphi(x_0). \tag{5.11}$$

Then $E\{Y_0|A\} = N[P_0 - AQ_0]$ yielding

$$\widehat{A} = \frac{P_0 - \widehat{P}_0}{Q_0} \qquad [\widehat{P}_0 = Y_0/N] \tag{5.12}$$

as an estimate of A. Remark H shows that $x_0 = 1$ is a reasonable choice, and derives the approximate standard error given A, yielding estimates

$$\textit{breast cancer}: \ \widehat{A} = 0.57 \pm 0.04, \qquad \textit{HIV}: \ \widehat{A} = -0.21 \pm .03 \tag{5.13}$$

for our two examples. For the breast cancer data, (5.13) implies $E\{Y(2.5)|\widehat{A}\} = 77$ and $\mathrm{Fdr}(2.5)|\widehat{A}) = 77/122 = 0.63$, underestimates according to our later calculations.

16

Permutation methods permit model-free estimates of the conditional Fdr, as in Figure 3 which suggests $E\{Y(2.5)|Y_0\} \doteq 118$, with corresponding estimated Fdr $118/122 = 0.97$.

Both of these approaches depend on the same basic idea: we use the observed central count Y_0 to condition the estimate of $Y(x)$, the unobserved null tail count. This is similar in spirit to Fisher's exact test for a 2×2 table, where the observed table margins, playing the role of Y_0, are used to establish the appropriate conditional null distribution.

The discussion so far has ignored the fact that not all N cases are null. Let N_0 be the actual number of nulls, so

$$p_o = N_0/N; \tag{5.14}$$

p_o is assumed to be large in the context of this paper, at least 0.90. We should really be dividing by N_0 rather than N in (5.12). Working back through the factors in (5.7)-(5.9), this error can substantially bias conditional Fdr estimates unless p_0 is very close to 1.0, perhaps $p_o \geq 0.98$.

Efron (2004) employs an estimate of central spread that does not depend on p_o. In terms of the histogram notation (2.2)-(2.3), suppose there are K_0 bins whose midpoints $z[k]$ lie within the interval $[-x_0, x_0]$, with $\mathcal{K}_0$ indicating the corresponding set of bin indices. The general linear model

$$y_k \overset{\text{ind}}{\sim} \text{Poisson}(\exp\{\beta_0 + \beta_1 z[k] + \beta_2 z[k]^2\}) \quad \text{for} \quad k \in \mathcal{K}_0 \tag{5.15}$$

yields maximum likelihood estimates $(\widehat{\beta}_0, \widehat{\beta}_1, \widehat{\beta}_2)$.

If we assume that null z-values have a $N(0, \sigma_0^2)$ distribution, that there are proportion p_o of them, and that the non-null counts fall mainly outside $[-x_0, x_0]$, then

$$E\{y_k\} \doteq N\Delta \frac{p_o}{\sqrt{2\pi\sigma_0^2}} \exp\left\{ -\frac{1}{2} \frac{z[k]^2}{\sigma_0^2} \right\} \tag{5.16}$$

for $k \in \mathcal{K}_0$. We see that β_2 equals $-1/2\sigma_0^2$ so that

$$\widehat{\sigma}_0 = 1/\sqrt{-2\widehat{\beta}_2} \tag{5.17}$$

efficiently estimates the central spread of the null z-values no matter what the value of p_o may be. (This is an example of "Lindsey's Method", described in Efron (2005) and Efron and Tibshirani (1996, Section 2). Efron (2004) shows that $\widehat{\sigma}_0$ has negligible bias for $p_o \geq 0.90$.) At this point we could take $\widehat{A} = (\widehat{\sigma}_0^2 - 1)/\sqrt{2}$ as in (3.16) and use (5.7)-(5.9), but it is simpler to estimate $Y(x)$ directly from $N\bar{\Phi}(x/\widehat{\sigma}_0)$, yielding conditional Fdr estimate

$$\text{Fdr}(x|\widehat{\sigma}_0) = N\bar{\Phi}(x/\widehat{\sigma}_0)/T(x). \tag{5.18}$$

Having estimated σ_0 in (5.16), we can also estimate the proportion of null cases p_o. Let

$$P_0(\sigma) = 2\Phi(x_0/\sigma_0) - 1, \tag{5.19}$$

so $P_0 = P_0(1)$ in (5.11). An estimate of p_o going back to Schweder and Spjotvoll (1982) is

$$\widehat{p}_o = \widehat{P}_0/P_0(\widehat{\sigma}_0) \qquad [\widehat{P}_0 = Y_0/N], \tag{5.20}$$

a version of the simplest possibility investigated in Langaas et al. (2005). Incorporating (5.20) into (5.18) gives an improved conditional Fdr estimate

$$\mathrm{Fdr}(x|\widehat{\sigma}_0) = N\widehat{p}_o\bar{\Phi}(x|\widehat{\sigma}_0)/T(x). \tag{5.21}$$

The equivalent unconditional estimate is

$$\mathrm{Fdr}_0(x) = N\widehat{p}_{oo}\bar{\Phi}(x)/T(x) \qquad \left[\widehat{p}_{oo} = \frac{\widehat{P}_0}{P_0(1)}\right], \tag{5.22}$$

(5.21) except with $\widehat{\sigma}_0$ replaced with 1, this being the theoretical null Fdr estimate corresponding to the empirical version (5.21).

Figure 5 reports on a small simulation experiment comparing (5.21) with (5.22). The simulation involved 200 trials, each with $N = 3000$ z-values, proportion $p_o = 0.95$ null. The null counts were generated from the Poisson model (3.15) with $\alpha = 0.15$, while the 150 non-null z's followed a $N(2.5, 1.25)$ distribution. Details appear in Remark F.

For each of the 200 trials, $\mathrm{Fdr}(x|\widehat{\sigma}_0)$ and $\mathrm{Fdr}_0(x)$, $x = 2.5$, are plotted versus the actual false discovery proportion (5.2). Strikingly, the unconditional estimate goes in the wrong direction, declining as the actual Fdp increases. This yields misleading inferences at both the low and high ends of the Fdp scale. The conditional estimate $\mathrm{Fdr}(x|\widehat{\sigma}_0)$ correctly tracks $\mathrm{Fdp}(x)$, though with a considerable amount of random noise.

Figure 5 validates the second main claim of the Introduction: correlation effects can and sometimes must be taken into account in the analysis of large-scale simultaneous testing problems. Not doing so may yield dangerously erroneous estimates of actual false discovery proportions.

To reiterate the basic idea, even assuming that null cases individually follow the theoretical null distribution $z_i \sim N(0, 1)$, correlation effects can make the ensemble null distribution behave more like $N(0, \sigma_0^2)$ with σ_0 surprisingly far from 1. Ignoring this effect can undercut any simultaneous testing procedure. Figure 6 concerns 1000 trials of the same simulation
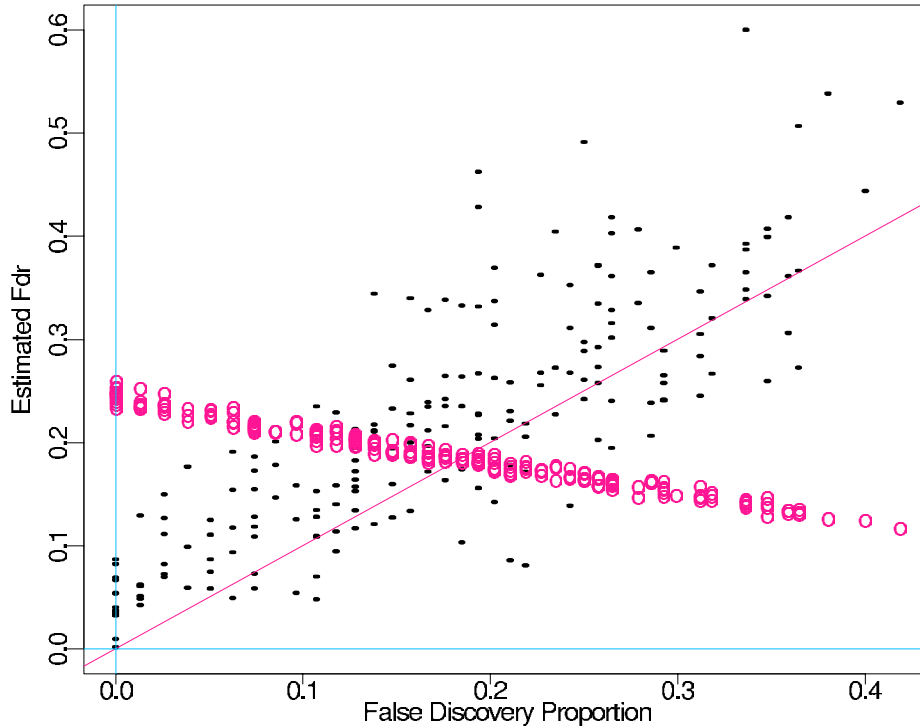
Figure 5: Simulation experiment comparing conditional Fdr estimates (5.21), solid points, with unconditional estimates (5.22), open circles; $N = 3000$, $p_o = 0.95$, $x = 2.5$. Null counts generated as in (3.15), $\alpha = 0.15$; non-null counts from $z \sim N(2.5, 1.25)$. Horizontal axis is actual False Discovery Proportion (5.2) for each of the 200 trials. The unconditional estimate, which is based on the theoretical null distribution, declines as actual Fdp increases..

used in Figure 5. The Benjamini-Hochberg (1995) FDR-controlling procedure, control parameter 0.10, was run for each trial, and the actual Fdp value (5.2) computed.

The overall mean of Fdp was 0.096, close to the theoretical control level, (even though the simulation model does not obey a correlation structure justifying the FDR algorithm, as in Benjamini and Yekutieli (2001) or Reiner et al. (2003)) but we see a strong dependence on the null dispersion parameter A, (3.15)-(3.16). Fdp averaged 0.34 for the upper 5% of A values, and 0.03 for the lower 5%. As in Figure 5, an estimate of A based on the observed central histogram counts, (5.15)-(5.17), can be used to correct the Benjamini-Hochberg inferences, so that Fdp averages about 0.10 across the range of A.

False discovery rates are convenient to analyze, but the same phenomena can be demonstrated for other simultaneous inference techniques. Remark K shows results like those in Figure 6 occurring with Lehmann and Romano's "kFWER" procedure, a generalization of the Family Wise Error Rate (2005).
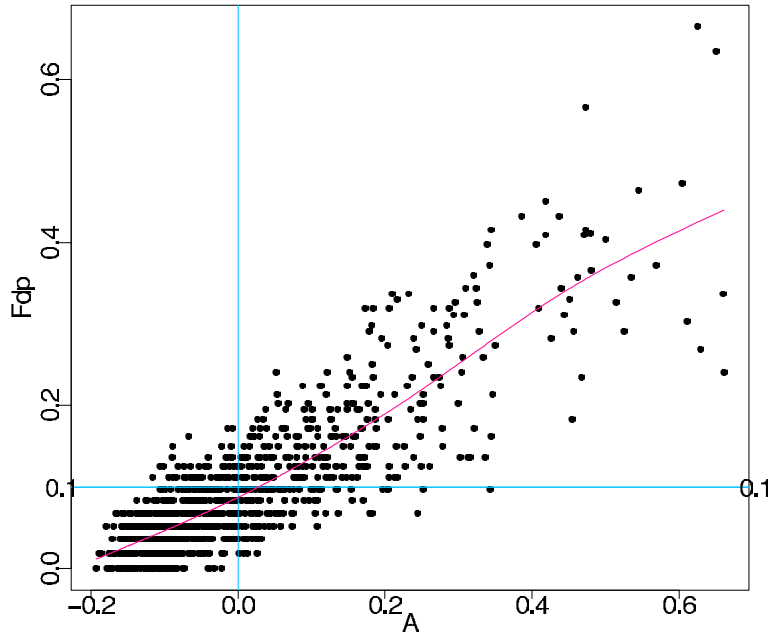
Figure 6: Benjamini-Hochberg FDR-controlling procedure, $q = 0.10$, run for 1000 trials of Figure 6's simulation; actual False Discovery Proportion Fdp, (5.2), for each trial plotted versus null dispersion parameter "A" (3.15)-(3.16). Overall Fdp averaged 0.096, close to q, but with a strong dependence on A, as shown by smooth regression curve..

The empirical null distributions (1.3) were obtained from "locfdr", a version of (5.15) that estimates the mean as well as the variance of the null, Efron (2004, 2005), (available as an R function from the Comprehensive R Archive Network.) Estimating the null distribution can be worrisomely noisy, as seen in Figure 5, where it is still preferable to depending on the theoretical null.

There is a lot at stake here. Table 3 shows the number of gene discoveries identified by the Benjamini-Hochberg two-sided procedure, FDR control level $q = 0.10$, for the two studies of Figure 1. The HIV results look much more dramatic using the empirical null distribution $N(-0.11, 0.75^2)$. In fact a null standard deviation of $\sigma_0 = 0.75$ is quite believable given the amount of correlations in (2.17), while Figure 1 argues against the theoretical null.

The breast cancer data has been used in the microarray literature to compare analysis techniques, under the presumption that better techniques will produce more discoveries, recently for instance in Pawitan et al. (2005) and Storey et al. (2005). Table 2 suggests caution in the interpretation, where using the empirical null negates any discoveries at all. (Part of the disagreement concerns this paper's focus on large values at p_o, see Remark I.) The theory of this paper is intended to show why correlation effects might support such a

	breast cancer	HIV
Theoretical Null:	107	22
Empirical Null:	0	180

Table 3:   Number of genes identified as significant discoveries by two-sided Benjamini-Hochberg procedure, 0.10 control level. *Top row* based on theoretical $N(0,1)$ null distribution; *Bottom row* using empirical null distribution (1.3).

negative conclusion, even if one is skeptical about the particular methodology behind (1.3).

Other factors besides z-value correlations can affect the null distribution. Efron (2004, 2005) suggests two other possibilities: unidentified covariates in an observational study, and correlations *across* microarrays. In fact, Figure 3 makes it seem unlikely that correlation effects alone are responsible for the extreme central overdispersion. These factors, as well as correlation, argue against uncritical use of theoretical null distributions in large-scale testing problems.

6.   Discussion   Massive data sets like those from the breast cancer and HIV studies can be misleadingly comforting in their suggestion of great statistical accuracy. Correlation considerations produce a more sobering picture. A single degree of freedom, embodied by the random variable A in (3.15), can dominate variability as it does in Table 1. Qui, Klebanov, and Yakovlev (2005) emphasize the harmful effect of correlation, using it as an argument against empirical Bayes microarray analyses such as those in Storey (2002) or Efron et al. (2001). Their arguments could be used just as well against all other popular microarray analysis techniques.

The results presented in this paper are more optimistic. The correlation effect, though perhaps very large, is shown to manifest itself via the simple wing-shaped function of Section 3. This enables the statistician to identify and remove much of it. In Figure 3, for example, the tail count Y_1 has standard deviation 15.5, much bigger than the value 4.5 applying to independent z_i's, but the standard deviation reduces to 6.5 after prediction from the central counts. This is the idea behind the empirical null, Efron (2004, 2005), whose most important job is predicting the conditional expectation of the tail null counts.

That being said, Qui et al.'s concern for the consequences of correlation on microarray analyses, nicely summarized in their Section 7, remains pertinent, especially in high-correlation settings like the HIV study. Improved biomedical methods in exposure, registration, and background control of arrays may alleviate the problem, as might new array designs

that incorporate greater gene duplication. Purely statistical improvements can also reduce correlations, for instance by more extensive standardization techniques as in Qui, Brooks, Klebanov, and Yakovlev (2005). None of this will help, however, if microarray correlations are inherent in the way genes interact at the DNA level, rather than a limitation of current methodology.

Not all large-scale testing situations involve microarrays. Correlation may be less of a problem in other scientific venues like fMRI imaging or time of flight spectroscopy. In any case it seems worthwhile to obtain some overall measure of correlation such as α, (3.2). Large α's suggest the use of correlation-resistant analysis techniques like the Fdr/empirical null combination.

7. Remarks

A (*Section 2*) Empirical correlation distributions (2.16)-(2.17) were obtained from the row-wise correlations of the original data matrix X, with X 3226×15 and 7680×8 in our two examples. Let $\widehat{\rho}_{ij}$ be the sample correlation between rows i and j of X, after first subtracting off each gene's average response within each treatment group (in order to nullify any genuine treatment differences); $g(\rho)$ is essentially the empirical distribution of all $N(N-1)/2$ $\widehat{\rho}_{ij}$ values, as in Owen (2005), but when dealing with small numbers of microarrays, only 15 or 8 points per correlation in our two examples, some care is needed to remove the variability added by sampling error. This was done by transforming to

$$\widehat{\xi}_{ij} = \frac{1}{2} \log \frac{1 + \widehat{\rho}_{ij}}{1 - \widehat{\rho}_{ij}}; \tag{7.1}$$

assuming a translation model $\widehat{\xi}_{ij} = \xi_{ij} + \epsilon$ on this scale; estimating the distribution of ϵ by repeating the calculations beginning with matrices X^* in which the entries within columns of X were independently permuted; inferring the ξ distribution by deconvolution; and retransforming back to the ρ scale. These calculations apply to the correlations within each column of X. Assuming independent columns, it is easy to demonstrate by simulation that nearly the same $g(\rho)$ distribution applies to the z-values (1.1).

B (*Section 2*) Owen's examples support normality for $g(\rho)$ as in (2.16), but a wide range of other distributions fit reasonably well. Table 4 shows the best distribution supported on just three ρ values. "Best" here is defined in terms of numerically minimizing a chi-square discrepancy between the empirical distribution of the $\widehat{\xi}_{ij}$ values and the model $\widehat{\xi} = \xi + \epsilon$, taking the ϵ distribution as above. The solution turned out to have mean 0 and standard deviation $\alpha = 0.153$, as in (2.16), and gave about the same estimate of cov($\mathbf{y}$) as (2.18).

$$\rho: \quad -0.250 \quad 0.000 \quad 0.444$$
$$g(\rho): \quad 0.131 \quad 0.793 \quad 0.076$$

Table 4:   Best 3-point distribution estimate for the breast cancer correlation density $g(\rho)$.

C (*Section 2*)   The amount of gene-wise correlation represented by (2.16) is enormous. For comparison, suppose that there were actually 10 equal sized groups of genes, with independence across groups but $\rho_{ij} = 0.50$ for all genes within groups. After standardization of X this gives $\alpha = 0.15$, about the same as (2.16).

D (*Section 3*)   The components of $\mathbf{u} = \boldsymbol{\nu} + A\mathbf{W}$ in (3.15) are

$$u_k \doteq N\Delta f_A(z[k]) \quad \text{where} \quad f_A(z) = \varphi(z) \cdot [1 + Aq(z)], \tag{7.2}$$

$q(z) = (z^2 - 1)/\sqrt{2}$, (2.7), (3.8); $f_A(z)$ is symmetric around zero, with even moments easily obtained from Hermite polynomial calculations,

$$\int_{-\infty}^{\infty} f_A(z)dz = 1, \quad \int_{-\infty}^{\infty} f_A(z)z^2 dz = 1 + \sqrt{2}A, \quad \int_{-\infty}^{\infty} f_A(z)z^4 dz = 3 + \frac{12}{\sqrt{2}}A. \tag{7.3}$$

This supports approximation (3.16), which can be improved upon using higher order Edgeworth terms.

E (*Section 3*)   The vectors $\boldsymbol{\nu}$ and $\mathbf{W}$ in (3.15) relate to the zeroth and second Hermite polynomials. Standardization of the columns of X suppresses the first polynomial, with important consequences here. Without standardization, the first eigenvector of $\text{cov}(\mathbf{y})$, divided by $\varphi(z)$, may be proportional to z, the first polynomial, instead of the second polynomial $z^2 - 1$.

F (*Section 4*)   The permutation calculations at the beginning of Section 4 provided 1000 z_i^* values for each index i, after which the empirical distribution of all 3226×1000 values provided the "permutation null" G_0. This kind of calculation ignores correlation among the z_i's since it only depends on marginal permutation distributions. It is worth restating that permutation null distributions as typically computed tend to resemble theoretical nulls, and do *not* automatically compensate for correlation effects. The sophisticated permutation algorithms of Westfall and Young (1993) and Westfall (1997) do involve gene-wise correlations, but applied toward different purposes than in this paper. Their "step-down max-T" algorithm gave results similar to using a $N(0,1)$ null for the breast cancer and HIV studies.

G (*Section 4*)   Permutation methods produced unstable results for the HIV data. Partly this reflects small sample sizes, with only 34 distinct permutations available. Of more concern, there seem to be secular effects systematically disturbing expression levels *across* microarrays, as described in Section 3 of Efron (2005). A version of Remark A based on random subsamples of the 7680 genes gave (2.17).

H (*Section 5*)   Linear functions of the count vector $\mathbf{y}$ yield useful estimates of A. For $\mathbf{m} = (m_1, m_2, \ldots , m_K)'$ define

$$\theta_m = \sum_k m_k u_k / N \quad \text{and} \quad \widehat{\theta}_m = \sum_k m_k y_k / N \tag{7.4}$$

in Poisson model (3.15). It is convenient to work with a continuous version of $\mathbf{m}$, say $m(z)$ where $m(z[k]) = m_k$. Letting

$$P_m = \int_{-\infty}^{\infty} m(z)\varphi(z)dz \quad \text{and} \quad Q_m = -\int_{-\infty}^{\infty} m(z)q(z)\varphi(z)dz \tag{7.5}$$

gives

$$\theta_m \doteq \int_{-\infty}^{\infty} m(z)f_A(z)dz = P_m - AQ_m \tag{7.6}$$

as in (7.2). If $m(z)$ is the indicator function of (x, ∞) then (7.6) becomes (5.7).

Since $E\{\widehat{\theta}_m | A\} = \theta_m$, (7.6) suggests

$$\widehat{A} = \frac{P_m - \widehat{\theta}_m}{Q_m} \tag{7.7}$$

as a method of moments estimator for A; (5.12) is (7.7) where $m(z)$ is the indicator function of $(-x_0, x_0)$, Model (3.15) then yields $\text{var}\{\widehat{\theta}_m | A\} \doteq \int f_A(z)m(z)^2 dz / N$ and

$$\text{var}\{\widehat{A}_m | A\} \doteq \frac{1}{N} \frac{\int_{-\infty}^{\infty} f_A(z)m(z)^2 dz}{(\int_{-\infty}^{\infty} \varphi(z)q(z)m(z)dz)^2}. \tag{7.8}$$

This formula, with A equaling 0.57 and -0.21 for the two studies, gave the standard errors in (5.13).

Suppose we wish to minimize (7.8) among functions $m(z)$ supported on $(-x_0, x_0)$. The formula is linear in A and in fact does not vary much across reasonable values of A. At $A = 0$, standard theory says that choosing $m(z)$ proportional to $q(z) = (z^2 - 1)/\sqrt{2}$ within $(-x_0, x_0)$ is optimal, the minimum variance equaling $[N \int_{-x_0}^{x_0} \varphi(z)q(z)^2 dz]^{-1}$. For $x_0 = 1$ this gives $\text{var}\{\widehat{A}_m | A = 0\} = 5.03/N$, compared to $1/N$ for $x_0 = \infty$, (the ideal choice but an

unallowable one given the possibility of biasing $\widehat{A}_m$ with non-null data). Taking $m(z)$ as the indicator of $(-1, 1)$ gives $5.83/N$. Reducing x_0 to 0.80 provides slightly smaller variance when $m(z)$ is the indicator, $5.36/N$. The more important point is that *conditional* variance estimates, as in (7.8), are both convenient and appropriate for the calculations here.

I (*Section 5*)   "A" $= 0$ in (3.15)-(3.16) corresponds to null counts following the $N(0, 1)$ theoretical null distribution. At $A = 0$ formula (7.8), with $x_0 = 1$ and optimal $m(z)$, gives conditional standard deviations

$$\textit{breast cancer } 0.040, \qquad \textit{HIV } 0.028, \tag{7.9}$$

making (5.13) strongly contradict the theoretical null.

As explained following (5.14), these standard errors are optimistically small in that they assume p_o very near 1. The GLM method (5.15) disposes with this assumption, at the cost of decreased efficiency: with $x_0 = 1$, $\widehat{\sigma}_0$ in (5.17) has about twice the standard error suggested by (7.9) and the relationship $\sigma_A \doteq 1 + A/\sqrt{2}$ from (3.16). A more daring choice, $x_0 = 1.5$, is necessary to get efficiency equivalent to (7.9).

J (*Section 5*)   All estimates of the null proportion p_o in the literature, such as $\widehat{p}_{oo}$ (5.22), assume correctness of the theoretical null distribution, Langlass et al. (2005). If it is not correct then methods that take the estimated null spread $\widehat{\sigma}_0$ into account, like $\widehat{p}_o$ (5.20), become necessary.

An important assumption of Section 5 is that p_o is large, $p_o \geq 0.9$, reflecting the usual goal in large-scale testing of winnowing an enormous class of possibilities down to a manageably small set of interesting cases. Efron (2004), shows that (5.17) will give nearly unbiased estimates of σ_0 when p_o exceeds 0.9. Langlass et al., using the theoretical null, estimate p_o as 0.67 for the breast cancer data, which is what $\widehat{p}_{oo}$ gives with $x_0 = 0.5$. Pawitan et al. (2005) suggest $p_o = 0.43$. Such small p_o values are necessary to explain the central spread of the breast cancer data assuming the theoretical null is correct. This paper suggests that correlation effects may undermine the theoretical null, and also the usual estimates of p_o. *Note*: the referee points out that a preliminary removal of "uninteresting cases" may sometimes decrease the apparent value of p_o, as in Ein-Dor et al. (2005). This is a dangerous tactic since the cases removed may contain valuable information concerning the null distribution.

For the HIV data, $\widehat{p}_{oo} = 1.19$ when $x_0 = 0.5$, reflecting the underdispersion seen in the right panel of Figure 1. Using the empirical null gives the sensible estimate $\widehat{p}_o = 0.93$.

K (*Section 5*)   Each point in Figure 5 and Figure 6 was calculated from the counts of a simulated vector of $N = 3000$ z-values, discretized into $K = 101$ bins of width 0.1 running from -4.1 to 6.0. Each count vector was constructed as follows: 150 non-null counts were obtained from an idealized $N(2.5, 1.25)$ distribution,

$$z_i = 2.5 + 1.25^{\frac{1}{2}}\Phi^{-1}((i - .5)/150) \qquad i = 1, 2, \dots, 150; \qquad (7.10)$$

null counts were generated according to model (3.15), with $N = 2850$, $\alpha = 0.15$, and the components of $\mathbf{u}$ truncated at zero; the values of A in (3.15) followed an idealized $N(0, \alpha^2)$ distribution.

The Fdr estimates in Figure 5 were obtained from (5.21) and (5.22). The calculation of $\widehat{\sigma}_0$ proceeded as in (5.15), (5.17), with one further correction. Because $\mathbf{u} = \boldsymbol{\nu} + A\mathbf{W}$, is not exactly proportional to $N(0, \sigma_A^2 = 1 + \sqrt{2}\ A)$ near $z = 0$, procedure (5.15)-(5.17) tends to be biased for estimating σ_0, as shown in Table 5. The mapping from (5.17) to σ_A in Table 5 was used to correct the value of $\widehat{\sigma}_0$ used in (5.21).

A	-0.40	-0.20	0	0.20	0.40
(5.17)	0.80	0.88	1	1.18	1.55
σ_A	0.66	0.85	1	1.13	1.25

Table 5:   Estimate (5.17) of σ_0 taking y_k proportional to $f_A(z[k])$, (7.2), in (5.15); compared to $\sigma_A = (1 + \sqrt{2}\ A)^{1/2}$.

The correction could be avoided by changing (5.15) to $Po(f_A(z[k])$ for $k \in \mathcal{K}_0$ and directly estimating A, but doing so requires special software since f_A is not an exponential family. This would be a worthwhile effort if correlation alone affected σ_0, but other causes such as unobserved covariates are possible, where f_A does not play a dominant role.

L (*Section 5*)   The fact that correlations can greatly widen or narrow the null distribution has to affect any simultaneous testing procedure, not only false discovery rates. The same simulation model used in Figures 5 and 6 was applied to Lehmann and Romano's (2005) "k-FWER" procedure, in this case calibrated to produce $k = 20$ or more false discoveries no more than 10% of the time. In Figure 7 the actual number of false discoveries for each replication is plotted against $\widehat{\sigma}_0$, its estimated null standard deviation. The k-FWER procedure performed conservatively, averaging less than 3 false discoveries per replication, with only 2 out of 400 exceeding $k = 20$. (The number of true discoveries was 39, 40, or 41 in all 400 trials, averaging 39.1.) As in Figure 6, the false discovery proportion was a strongly increasing function of $\widehat{\sigma}_0$, averaging .036 for $\widehat{\sigma}_0 \le 0.90$ and .224 for $\widehat{\sigma}_0 \ge 1.20$.
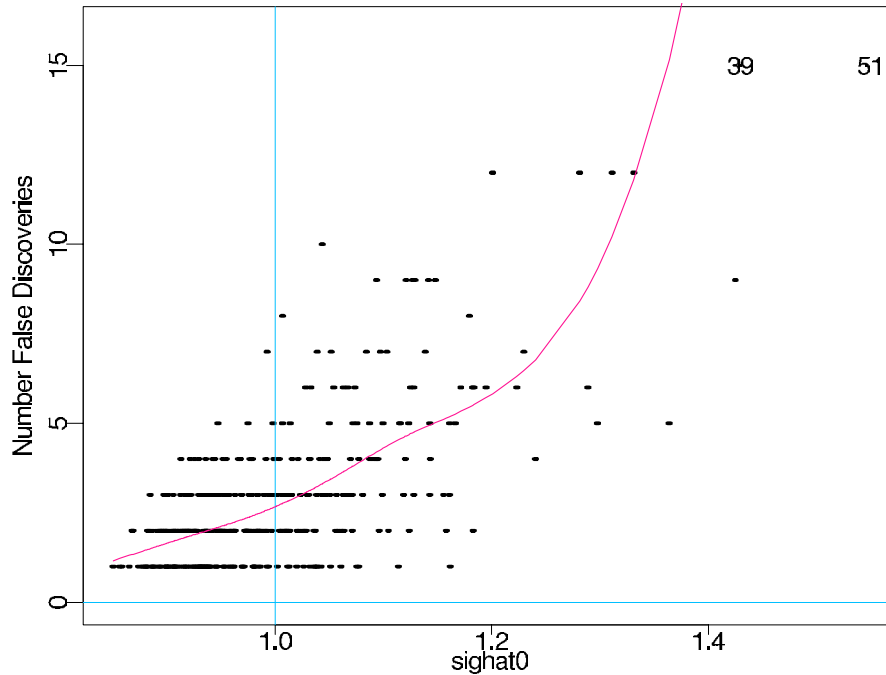
Figure 7: 400 replications of simulation model used in Figures 5 and 6 applied to Lehmann-Romano k-FWER procedure, $k = 20$, error control rate 0.1; number of false discoveries increase with $\widehat{\sigma}_0$, the null standard deviation. Two points at right had 39 and 51 false discoveries. Curve is smoothing spline..

References

Benjamini Y and Hochberg Y, (1995), Controlling the false discovery rate: A practical and powerful approach to multiple testing, *J.R. Stat. Soc. Ser. B Stat. Methodol.* **57**, 289-300.

Benjamini Y and Yekutieli D (2001), "The control of the false discovery rate under dependency", *Ann. Stat.* **29**, 1165-88.

Bolstad B, Irizarry R, Astrand M, Speed T, (2003), "A comparison of normalization methods for high density oligonucleotide array data based on variance and bias", *Bioinformatics* **19** (2):185-193.

Dudoit S, van der Laan M, and Pollard K (2004), "Multiple testing, Part I. Single-step procedures for control of general type I error rates", *Stat. Application in Genetics and Molecular Biology*, **3**, No. 1, Article 13.

Efron B and Tibshirani R (1996), "Using specially designed exponential families for density estimation", *Ann. Stat.* **24**, 2431-61.

Efron B, Tibshirani R, Storey J and Tusher V, (2001), Empirical Bayes analysis of a microarray experiment, *J. Amer. Statist. Assoc.* **96**, 1151-1160.

Efron B and Tibshirani R, (2002), "Empirical Bayes methods and false discovery rates for microarrays", *Genetic Epidemiology* **23**, 70-86.

Efron B, (2004), "Large-scale simultaneous hypothesis testing: the choice of a null hypothesis", *JASA* **99**, 96-104.

Efron B, (2005), "Local false discovery rates", http://www-stat.stanford.edu/ brad/papers/False.pdf

Ein-Dor L, Kela I, Geta G, Givol D, and Domany E (2005), "Outcome signature genes in breast cancer: is there a unique set?", *Bioinformatics* **21**, 171-78.

Ge Y, Dudoit S, Speed T, (2003), "Resampling-based multiple testing for microarray data analysis (with comments), *TEST* **12**, 1-77.

Hedenfalk I, Duggen D, Chen Y, et al. (2001), "Gene expression profiles in hereditary breast cancer", *New Engl. Jour. Medicine* **344**, 539-48.

Ishwaran H and Rao JS (2003), "Detecting differentially expressed genes in microarrays using Bayesian model selection", *JASA* **98**, 438-55.

Lanaas M and Lindquist B (2005), "Estimating the proportion of true null hypotheses, with application to DNA microarray data", *JRSS-B* **67**, 555-72.

Lehmann E and Roman J (2005), "Generalizations of the Familywise Error Rate", *Annals Stat.* **33** , 1138-1154.

Owen A, (2005), "Variance of the number of false discoveries", *JRSS-B* **67**, 411-26.

Pawitan Y, Murthy K, Michiels S, and Ploner A (2005), "Bias in the estimation of false discovery rate in microarray studies", *Bioinformatics* **21**, 3865-72.

Qui, X, Klebanov L, Yakovlev A, (2005), "Correlation between gene expression levels and limitations of the empirical Bayes methodology in microarray data analysis", *Statistical Applications in Genetics and Molecular Biology* **4**, Issue 1, Paper 34.

Qui X, Brooks A, Klebanov L, Yakovlev A, (2005), "The effects of normalization on the correlation structure of microarray data", *BMC Bioinformatics* **6:120** {b} 2005-05-16.

Reiner A, Yekutieli D, and Benjamini Y (2003), "Identifying differentially expressed genes using false discovery rate controlling procedures", *Bioinformatics* **19**, 368-75.

Schweder T and Spjotvoll E (1982), "Plots of p-values to evaluate many tests simultaneously", *Biometrika* **69**, 493-502.

Storey J, (2002), "A direct approach to false discovery rates", *JRSS-B* **64**, 479-498.

Storey J, Taylor J, Siegmund D, (2004), "Strong control, conservative point estimation, and simultaneous conservative consistency of false discovery rates: a unified approach", *JRSS-B* **66**, 187-205.

Storey J, Dai J, and Leek J (2005), "The optimal discovery procedure II: applications to comparative microarray experiments", http://www.bepress.com/uwbiostat/paper260.

van't Wout A, Lehrma G, Mikheeva S, O'Keeffe G, Katze M, Bumgarner R, Geiss G, and Mullins J, (2003), "Cellular gene expression upon human immunodeficiency virus type 1 infection of CD\$+ T-Cell lines", *Journal of Virology* **77**, 1392-1402.

Westfall P and Young S, (1993), *Resampling-based multiple testing: examples and methods for p-value adjustments.* Wiley, New York.

Westfall P (1997), "Multiple testing of general contrasts using logical constraints and correlations", *JASA* **92**, 299-306.